AIP Journal of Applied Physics

Hysteresis and mode transitions in plasma sheath collapse due to secondary electron emission

Samuel Langendorf and Mitchell Walker

Citation: Journal of Applied Physics **119**, 113305 (2016); doi: 10.1063/1.4943778
View online: http://dx.doi.org/10.1063/1.4943778
View Table of Contents: http://scitation.aip.org/content/aip/journal/jap/119/11?ver=pdfcov
Published by the AIP Publishing

JOURNAL OF APPLIED PHYSICS **119**, 113305 (2016)

Hysteresis and mode transitions in plasma sheath collapse due to secondary electron emission

Samuel Langendorf[a)] and Mitchell Walker[b)]
School of Aerospace Engineering, Georgia Institute of Technology, Atlanta, Georgia 30332, USA

(Received 2 December 2015; accepted 1 March 2016; published online 21 March 2016)

In this experiment, hysteresis is observed in the floating potential of wall material samples immersed in a low-temperature plasma as the energy of a prevalent non-thermal electron population is varied from 30–180 eV. It is indicated that the hysteresis is due to secondary electron emission from the wall material surface. Measurements are performed in a filament discharge in argon gas pressure 10^{-4} Torr of order 10^{7} cm^{-3} plasma number density. The primary ionizing electrons from the discharge filament make up 1%–10% of the overall plasma number density, depending on discharge voltage. Immersed LaB_6-coated steel and roughened boron nitride (BN) wall material samples are mounted on the face of a radiative heater, and the wall temperature is controlled from 50–400 °C such that thermionic emission from the LaB_6-coated sample is not significant. The energy of the primary plasma electrons from the discharge filament is varied and the floating potentials of the material samples are monitored. The floating potentials are observed to transition to a "collapsed" state as the primary electron energy is increased above 110 and 130 eV for the LaB_6 and rough BN, respectively. As primary electron energy is subsequently decreased, the floating potentials do not "un-collapse" until lower energies of 80 and 100 eV, respectively. The hysteresis behavior agrees with a kinetic model. The results may help explain observations of global hysteresis and mode transitions in bounded plasma devices with dielectric walls, significant secondary electron emission, and departures of electron energy distribution function from a thermal Maxwellian. © *2016 AIP Publishing LLC*. [http://dx.doi.org/10.1063/1.4943778]

I. INTRODUCTION

Hysteresis and mode-shifting behavior has been reported in a wide variety of bounded plasma devices, including thermionic filament discharges,[1] magnetized linear plasmas,[2,3] radio-frequency-driven discharges,[4–6] and Hall effect thrusters.[7,8] A number of mechanisms for the observed behavior have been theorized (see, e.g., Ref. 4), many having to do with the electron power balance and energy flux to and from the device walls, as mediated by the nonlinear plasma sheath.

Experimental investigations by Takamura *et al.*[3] focused on the plasma-wall interaction and sheath in high-heat-flux plasmas revealed and explained a clear wall-dependent mechanism for hysteresis in the wall floating potential driven by thermionic electron emission from the wall. It is shown that when the plasma heats the wall to a sufficient temperature, thermionic electron emission from the wall causes a space-charge collapse of the magnitude of the sheath potential to the order of the electron temperature or lower/inverse, as described originally by Hobbs and Wesson[9] and recently by Campanell[10] and Sheehan.[11] With the decrease in sheath potential, the electron heat flux to the wall is increased, thereby again increasing thermionic electron emission from the wall. This creates a feedback mechanism and the sheath floating potential and wall temperature shift to a new "collapsed sheath" equilibrium. At a later time, if the heat flux from the plasma is then lowered, Takamura *et al.* observe that the sheath often remains collapsed at lower values of the plasma heat flux than were required to collapse it in the first place. Because the sheath potential has been collapsed, the wall is still receiving elevated heat flux from the plasma and generates enough thermionic electron emission to keep the sheath collapsed. If the heat flux is lowered below a threshold dependent on the wall material work function, the electron emission will become insufficient to maintain the collapsed sheath and the Debye sheath will be re-established. This mechanism explains observed hysteresis in plasmas where thermionic components are employed and heat flux from the plasma is significant.

Several plasma devices that exhibit hysteresis employ dielectric boundaries from which secondary electron emission (SEE) is significant. SEE was theorized to give rise to multi-valued floating potentials of cosmic dust grains in a work by Meyer-Vernet.[12] In first experiments by Nam *et al.*,[13] abrupt jumps were observed in the floating potential of Langmuir probes in a multidipole plasma, and inferred the existence of multiple stable floating potentials of the probe. Work by Walch *et al.*[14] observed sharp transitions in floating potential of dust grains in response to an energetic electron population. These results suggest that SEE may play an important role in mode-shifts and/or hysteresis in plasma devices as well.

In the current experiment, we monitor floating potential of macroscopic wall material samples as the energy of a beam-like electron population is either increased or decreased. This allows us to observe full hysteresis curves of

a)Electronic mail: samuel.langendorf@lanl.gov
b)Electronic mail: mitchell.walker@ae.gatech.edu

the sample floating potentials. We compare results with a kinetic model[15] and find agreement with a nonlinear s-curve shape prediction of floating potential, similar to the predictions of Meyer-Vernet.[12]

II. EXPERIMENTS

Experiments are conducted in an open cylindrical multi-dipole plasma device in the Vacuum Test Facility-2 at the Georgia Institute of Technology. Fig. 1 shows a schematic of the device and experimental layout. The discharge is operated at an argon gas pressure of 10^{-4} Torr-Ar. The discharge voltage is applied between the hot filaments and the electrically grounded aluminum frame. The discharge current is restrained to 10 mA by limiting the heating current and temperature of the filaments, to attain a plasma density n_e on the order of 10^7 cm^{-3} and a significant fraction of energetic electrons n_{ep} from the filament present in the plasma. The energy of the energetic electrons from the filament is varied by changing the discharge voltage, from 50–200 V in this experiment. The fraction of energetic electrons $\alpha = n_{ep}/n_e$ was measured using a planar Langmuir probe and the method described in Ref. 16, shown in Fig. 2.

A. LaB_6-coated steel material sample

Three-inch diameter wall material samples are mounted on a 4.5 in.-side cube-shaped sample heater, suspended in the plasma device opposite the discharge filaments. The heater contains coils of heating wire wrapped around ceramic tubing. The stainless steel body of the heater is electrically isolated from the device frame by a ceramic standoff on its mounting rod. The focus of this part of the experiment was on a LaB_6-coated steel wall material sample. The sample is stood off 1/8 in. from the heater face by ceramic standoffs and the perimeter gap is filled with ceramic adhesive. It is thus electrically isolated from the heater body and can be heated radiatively from the heating elements. A wire was

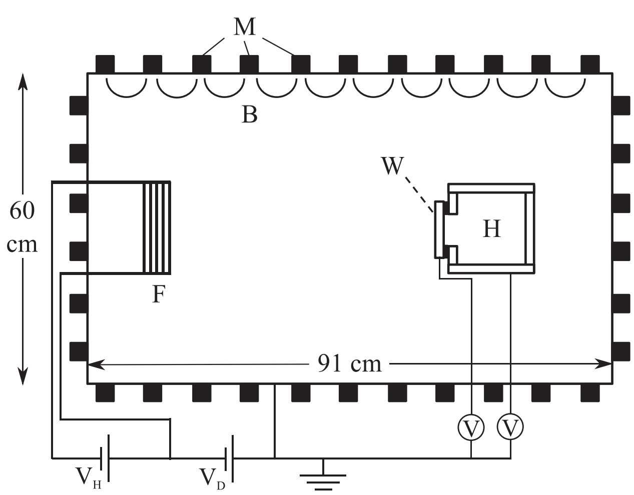

FIG. 1. Schematic of the plasma device and experimental layout. M = magnets, B = notional magnetic field, F = filament cathode, W = wall material sample, H = heater volume, V_D = discharge power supply, and V_H = filament heater power supply.

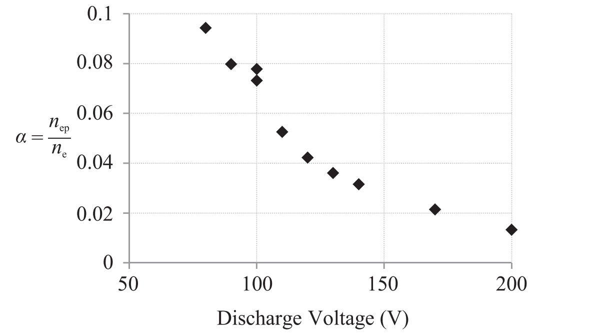

FIG. 2. Measured fraction of energetic primary electrons $\alpha = n_{ep}/n_e$ in plasma 100 mm from wall material sample vs. discharge voltage. Relative uncertainty is less than 20%, absolute uncertainty is estimated at a factor of two.

connected to the sample, and its floating potential was measured with a 10 MΩ-impedance ADC channel.

The discharge voltage of the plasma device is varied from 50 to 200 V at a rate of approximately 1 V/s, while the floating potential of the wall material sample is monitored, as shown in Fig. 3. The plasma potential remains fairly constant at −21 V, so the primary electron energy is offset from the discharge voltage by this amount but scales linearly with it. Fig. 4 plots the results of the floating potential of the wall material sample vs discharge voltage. The discharge voltage sweep from 50 to 200 V is repeated for heater powers from 170 W to 560 W and resulting average wall temperatures 55 °C to 390 °C. The discharge voltages at which the abrupt changes in floating voltage occur are plotted in Fig. 5, in which it is observed that as the heater power and wall temperature is increased, the hysteresis loop in wall floating potential gradually shrinks and disappears. Concurrently with the disappearance of the hysteresis in floating potential, a glow is observed within the sample heater box, leading the experimenters to infer that a plasma forms inside the box at these conditions. Supporting this belief, it is observed that the floating potential of the metal sample heater box and the LaB_6-coated steel sample under investigation become the same at temperatures above 450 °C, even if the sample is electrically biased using the attached lead.

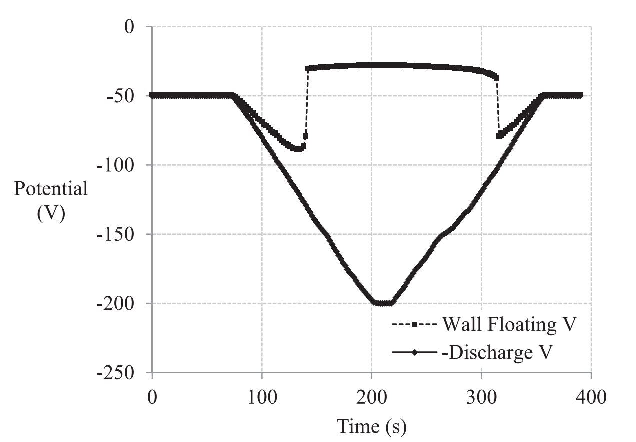

FIG. 3. Floating potential of LaB_6-coated steel wall material sample in plasma and discharge voltage vs time as discharge voltage is varied. The wall temperature is 50 °C.

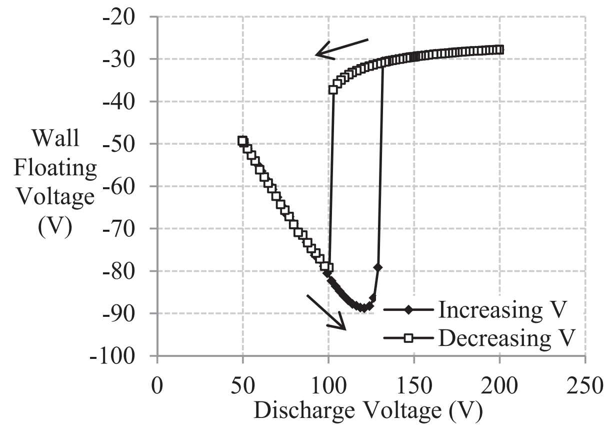

FIG. 4. Floating potential of LaB_6-coated steel wall material sample vs. discharge voltage. The wall temperature is 50 °C.

B. Boron nitride (BN) sample

Experiments are continued with a roughened BN ceramic sample of equivalent dimensions. The sample had been utilized in previous experiments to do with surface roughness and had been prepared by sanding with 120-grit SiC paper to an average roughness of 10 μm. As the sample is not electrically conductive, the floating potential could not be monitored by a simple wire as previously. A small 1-mm half-loop electrostatic probe was positioned on the surface of the device to monitor the floating potential. The probe tip was 0.005 in. diameter thoriated tungsten, and it was supported by a double-bore alumina tube. As the probe formed a small amount of the collecting area with a circle with radius equal to the plasma Debye length (which varied from 7 to 9 mm) on the sample surface, it was reasoned that the floating potential of the probe would be largely governed by the potential of the nearby BN surface. To confirm this, the probe was positioned over the LaB_6 sample, and the probe potential was monitored along with that sample, as shown in Fig. 6.

Positioning the probe over the rough BN sample, the floating potential of the probe was monitored in a similar study to the LaB6 sample. The results are shown in Figs. 7 and 8.

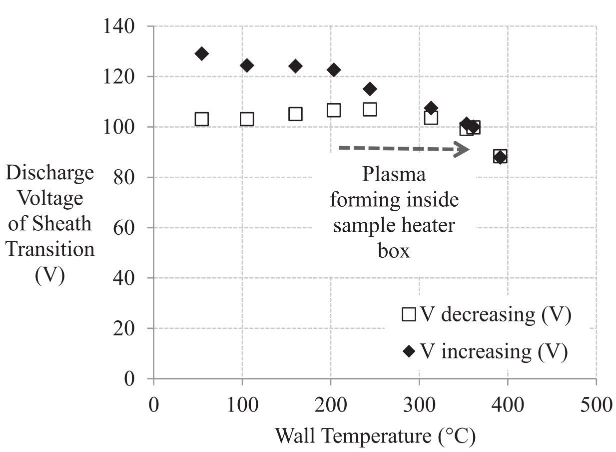

FIG. 5. Transition voltages in wall floating potential vs wall temperature. Glow observed within heater volume concurrently with disappearance of hysteresis.

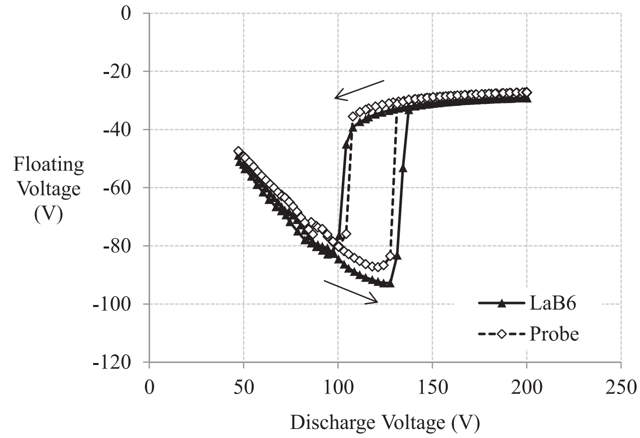

FIG. 6. Floating potential of LaB_6-coated steel wall material sample and adjacent probe vs. discharge voltage. The wall temperature is 50 °C.

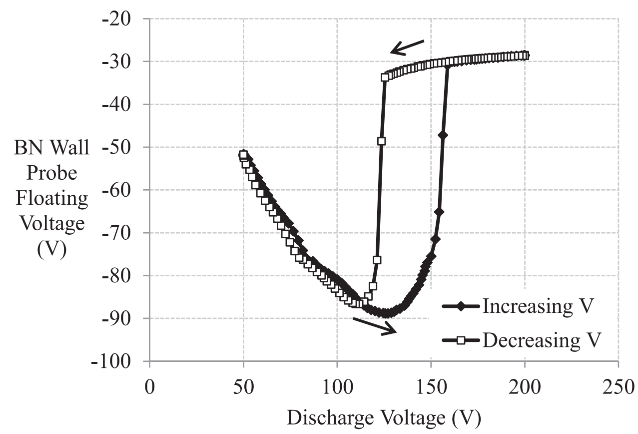

FIG. 7. Floating potential of witness probe adjacent to BN sample vs. discharge voltage. The wall temperature is 50 °C.

III. DISCUSSION

At low discharge voltages, the wall floating voltage is very close to the discharge voltage (Fig. 3). This is due to the considerable prevalence of the energetic electrons in these conditions (Fig. 2)—in order to satisfy the floating condition, the wall must repel almost all of the energetic electrons to equate their flux with the ion flux and thus must approximately match the discharge voltage. As the discharge

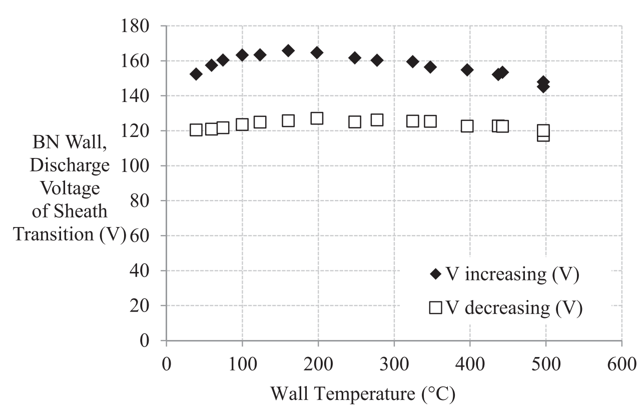

FIG. 8. Transition voltages in floating potential of witness probe adjacent to BN sample vs. wall temperature.

voltage/primary electron energy increases, the prevalence decreases and the wall is able to collect a larger fraction of the energetic electrons, and as such the floating voltage becomes increasingly separated from the discharge voltage.

As the discharge voltage is further increased, a sharp change is observed in wall floating voltage. This change indicates a space-charge sheath collapse, which is not unexpected as the wall had been collecting increased energetic electron energy and flux. The wall temperature is always well below that expected for significant thermionic emission from LaB_6, and the heat flux from the plasma is also low given the order $10^7\,\mathrm{cm}^{-3}$ density, so the electron emission mechanism causing the collapse must be SEE rather than thermionic emission. This collapse of the sheath potential allows the energetic electrons to impact the wall with increased energy, no longer slowed by the retarding sheath voltage. This appears to be the root cause of the observed hysteresis—once the sheath potential is collapsed, plasma electrons are able to impact the wall with increased energy and generate a greater secondary electron yield. The effect is to create a feedback mechanism and hysteresis similar to that observed by Takamura *et al.*, so when the plasma electron energy is again decreased, the sheath voltage is not restored until the electron energy is decreased substantially below that required to cause the collapse.

As the heater power is increased, a plasma is generated inside the heater box, and it is observed that the size of the hysteresis loop decreases and disappears. Although electrically isolated in vacuum, the LaB_6-coated wall material sample is uninsulated over most of its area facing the interior of the heater, and is thus able to receive plasma flux from both sides if there is plasma within the heater volume. The observed impact on the floating potential agrees with the prediction that a certain prevalence of energetic electrons is required for the hysteresis to occur, reasoning that the energies of the electrons in the plasma interior to the box are likely low and that as their number increases, the effective energetic electron prevalence α experienced by the wall material sample decreases.

To more explicitly evaluate the measured floating potentials, the measured potentials of the BN wall are plotted against predictions of the model from Ref. 15. Results are shown in Fig. 9. Average experimental values of $\alpha = 0.03$ and $T_e = 3\,\mathrm{eV}$ are used in input to the model (imperfect as the experimental value of α changes as the discharge voltage is varied, cf. Fig. 2), along with SEE data from literature measurements of clean BN.[17] It is observed that the sheath collapses at higher voltages for the roughened BN sample, as it obstructs SEE by geometric obstruction. Adjusting the input SEE yield to the model, it is observed that the transition occurs at about the right voltages when the SEE yield is 70% of the literature value. This view also makes it apparent that the physically observed behavior corresponds to "falling off" the two stable branches of the s-curve solution, accounting for the observed abrupt changes in floating potential and the hysteresis loop.

The full description of SEE yield with incident energy is not linear; at much higher energies it begins to decrease with incident energy.[18] Outcomes in those higher energy regimes

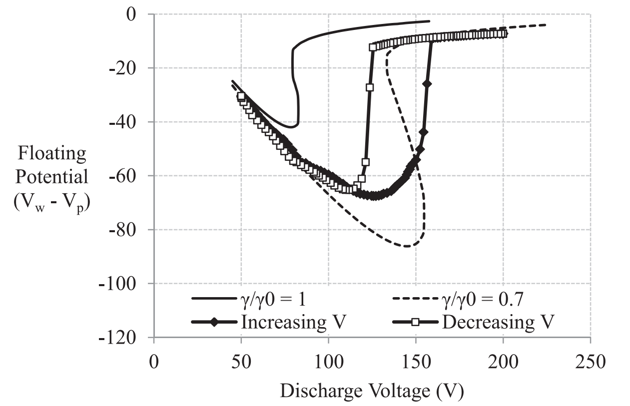

FIG. 9. Comparison between observed floating potentials of rough BN wall and model of Ref. 15 using average experimental values of $\alpha = n_{ep}/n_e = 0.03$ and $T_e = 3\,\mathrm{eV}$.

may be interesting to study and differ from the current experiments, which are firmly within the regime where SEE yield increases with incident energy.

IV. CONCLUSIONS

It is confirmed that a hysteresis in the plasma-wall interaction can occur in low-heat-flux plasmas when an energetic electron population is present. The hysteresis is precipitated by modification of the plasma electron energy distribution function (EEDF) by the acceleration of an energetic electron population. Distinct hysteresis curves have been measured experimentally. The effect of non-thermal electron populations as a cause for hysteresis and mode-shifts in many devices has not been greatly explored, though non-thermal EEDF's have been identified or are suspected in many of the devices in which mode-shifting behavior is observed.[19,20] The mechanism identified in the current investigation may play a role in explaining observed hysteresis and mode-shifting behavior in plasma devices with dielectric walls and significant SEE in cases where there is significant deviation of the plasma EEDF from a thermal Maxwellian.

ACKNOWLEDGMENTS

This work was supported by the Air Force Office of Scientific Research through Grant No. FA9550-11-10160.

[1] R. Timm and A. Piel, Contrib. Plasma Phys. **32**, 599 (1992).
[2] S. Takamura, N. Ohno, K. Shiraishi, and S. Masuzaki, J. Nucl. Mater. **196–198**, 448 (1992).
[3] M. Ye, S. Masuzaki, K. Shiraishi, S. Takamura, and N. Ohno, Phys. Plasmas **3**, 281 (1996).
[4] M. Turner and M. Lieberman, Plasma Sources Sci. Technol. **8**, 313 (1999).
[5] S. Xu, K. Ostrikov, W. Luo, and S. Lee, J. Vac. Sci. Technol. A **18**, 2185 (2000).
[6] S. Singh, J. Appl. Phys. **103**, 83303 (2008).
[7] M. J. Sekerak, B. W. Longmier, A. D. Gallimore, D. L. Brown, R. R. Hofer, and J. E. Polk, "Mode Transitions in Hall Effect Thrusters," AIAA Paper No. 2013-4116, 2013.
[8] D. L. Brown, "Investigation of low discharge voltage Hall thruster characteristics and evaluation of loss mechanisms," Ph.D. thesis (University of Michigan, 2009).
[9] G. Hobbs and J. Wesson, Plasma Phys. **9**, 85 (1967).
[10] M. Campanell, Phys. Plasmas **22**, 040702 (2015).
[11] J. Sheehan, I. Kaganovich, H. Wang, D. Sydorenko, Y. Raitses, and N. Hershkowitz, Phys. Plasmas **21**, 063502 (2014).

[12]N. Meyer-Vernet, Astron. Astrophys. **105**, 98 (1982).
[13]C.-H. Nam, N. Hershkowitz, M. Cho, T. Intrator, and D. Diebold, J. Appl. Phys. **63**, 5674 (1988).
[14]B. Walch, M. Horányi, and S. Robertson, Phys. Rev. Lett. **75**, 838 (1995).
[15]S. Langendorf and M. Walker, Phys. Plasmas **22**, 033515 (2015).
[16]N. Hershkowitz, J. R. DeKock, P. Coakley, and S. L. Cartier, Rev. Sci. Instrum. **51**, 64 (1980).
[17]J. P. Bugeat and C. Koppel, in *Proceedings of the 23rd International Conference on Electric Propulsion, IEPC* (1995), pp. 95–35.
[18]A. Shih, J. Yater, C. Hor, and R. Abrams, Appl. Surf. Sci. **111**, 251 (1997).
[19]V. Godyak, R. Piejak, and B. Alexandrovich, Plasma Sources Sci. Technol. **11**, 525 (2002).
[20]D. Sydorenko, A. Smolyakov, I. Kaganovich, and Y. Raitses, Phys. Plasmas **13**, 014501 (2006).